Biomedical Optics EXPRESS

Smartphone instrument for portable enzyme-linked immunosorbent assays

Kenneth D. Long,[1] Hojeong Yu,[2] and Brian T. Cunningham[1,2,*]

[1]*Department of Bioengineering, Micro and Nanotechnology Laboratory, University of Illinois at Urbana-Champaign, 208 N. Wright Street, Urbana, IL, 61801, USA*

[2]*Department of Electrical and Computer Engineering, Micro and Nanotechnology Laboratory, University of Illinois at Urbana-Champaign, 208 N. Wright Street, Urbana, IL, 61801, USA*

[*]*bcunning@illinois.edu*

Abstract: We demonstrate the utilization of a smartphone camera as a spectrometer that is capable of measuring Enzyme Linked Immunosorbent Assays (ELISA) at biologically-relevant concentrations with the aid of a custom cradle that aligns a diffraction grating and a collimating lens between a light source and the imaging sensor. Two example biomarkers are assayed using conventional ELISA protocols: IL-6, a protein used diagnostically for several types of cancer, and Ara h 1, one of the principle peanut allergens. In addition to the demonstration of limits of detection at medically-relevant concentrations, a screening of various cookies was completed to measure levels of peanut cross-contamination in local bakeries. The results demonstrate the utility of the instrument for quantitatively performing broad classes of homogeneous colorimetric assays, in which the endpoint readout is the color change of a liquid sample.

OCIS codes: (280.1415) Biological sensing and sensors; (280.4788) Optical sensing and sensors; (300.1030) Absorption.

References and links

1. A. Son, "Diagnostic & Medical Laboratories in the US industry report," (IBISWorld, 2013).
2. M. J. Dill, and S. E. Salsberg, "The Complexities of Physician Supply: Projections Through 2025," (Center for Workforce Studies, 2008).
3. A. L. Litster, B. Pressler, A. Volpe, and E. Dubovi, "Accuracy of a point-of-care ELISA test kit for predicting the presence of protective canine parvovirus and canine distemper virus antibody concentrations in dogs," Vet. J. **193**(2), 363–366 (2012).
4. R. G. Norkus, J. Maurer, N. A. Schultz, J. D. Stuart, G. A. Robbins, and R. D. Bristol, "Field examination of ground water quality as an indicator of microbiological activity at gasoline contaminated sites," Chemosphere **33**(3), 421–436 (1996).
5. G. Bansal, W. Zhou, P. J. Barlow, P. S. Joshi, H. L. Lo, and Y. K. Chung, "Review of rapid tests available for measuring the quality changes in frying oils and comparison with standard methods," Crit. Rev. Food Sci. Nutr. **50**(6), 503–514 (2010).
6. R. Suebsing, J. Kampeera, B. Tookdee, B. Withyachumnarnkul, W. Turner, and W. Kiatpathomchai, "Evaluation of colorimetric loop-mediated isothermal amplification assay for visual detection of Streptococcus agalactiae and Streptococcus iniae in tilapia," Lett. Appl. Microbiol. **57**(4), 317–324 (2013).
7. T. I. Day, Brent, "Global Analysis of the Smartphones Market: Who's Winning the Necessary Regional Battles," (2013).
8. G. Comtois, J. I. Salisbury, and Y. Sun, "A smartphone-based platform for analyzing physiological audio signals," in *Bioengineering Conference (NEBEC), 2012 38th Annual Northeast*, 2012), 69–70.
9. C. C. Huang, P. Y. Lee, P. Y. Chen, and T. Y. Liu, "Design and implementation of a smartphone-based portable ultrasound pulsed-wave doppler device for blood flow measurement," IEEE Trans. Ultrason. Ferroelectr. Freq. Control **59**(1), 182–188 (2012).
10. D. N. Breslauer, R. N. Maamari, N. A. Switz, W. A. Lam, and D. A. Fletcher, "Mobile phone based clinical microscopy for global health applications," PLoS ONE **4**(7), e6320 (2009).
11. Q. Wei, H. Qi, W. Luo, D. Tseng, S. J. Ki, Z. Wan, Z. Göröcs, L. A. Bentolila, T.-T. Wu, R. Sun, and A. Ozcan, "Fluorescent Imaging of Single Nanoparticles and Viruses on a Smart Phone," ACS Nano **7**(10), 9147–9155 (2013).
12. D. Gallegos, K. D. Long, H. Yu, P. P. Clark, Y. Lin, S. George, P. Nath, and B. T. Cunningham, "Label-free biodetection using a smartphone," Lab Chip **13**(11), 2124–2132 (2013).

#212166 - $15.00 USD Received 15 May 2014; revised 28 Aug 2014; accepted 29 Sep 2014; published 1 Oct 2014

13. R. M. Lequin, "Enzyme immunoassay (EIA)/enzyme-linked immunosorbent assay (ELISA)," Clin. Chem. **51**(12), 2415–2418 (2005).
14. L. Shen, J. A. Hagen, and I. Papautsky, "Point-of-care colorimetric detection with a smartphone," Lab Chip **12**(21), 4240–4243 (2012).
15. A. F. Coskun, J. Wong, D. Khodadadi, R. Nagi, A. Tey, and A. Ozcan, "A personalized food allergen testing platform on a cellphone," Lab Chip **13**(4), 636–640 (2013).
16. Q. Wei, R. Nagi, K. Sadeghi, S. Feng, E. Yan, S. J. Ki, R. Caire, D. Tseng, and A. Ozcan, "Detection and Spatial Mapping of Mercury Contamination in Water Samples Using a Smart-Phone," ACS Nano **8**(2), 1121–1129 (2014).
17. D. J. Guerrero, W. DiMenna, T. D. Flaim, R. Mercado, and S. Sun, "Dyed red, green, and blue photoresist for manufacture of high-resolution color filter arrays for image sensors," in 2003), 298–306.
18. H. Eliasson, "Color calibration of a CMOS digital camera for mobile imaging," in *Society of Photo-Optical Instrumentation Engineers (SPIE) Conference Series*, Society of Photo-Optical Instrumentation Engineers (SPIE) Conference Series (Society of Photo-Optical Instrumentation Engineers (SPIE) Conference Series, 2010), 753709–753711.
19. J. Kai, A. Puntambekar, N. Santiago, S. H. Lee, D. W. Sehy, V. Moore, J. Han, and C. H. Ahn, "A novel microfluidic microplate as the next generation assay platform for enzyme linked immunoassays (ELISA)," Lab Chip **12**(21), 4257–4262 (2012).
20. F. Poulsen and K. B. Jensen, "A luminescent oxygen channeling immunoassay for the determination of insulin in human plasma," J. Biomol. Screen. **12**(2), 240–247 (2007).
21. E. Cauchon, S. Liu, M. D. Percival, S. E. Rowland, D. Xu, C. Binkert, P. Strickner, and J.-P. Falgueyret, "Development of a homogeneous immunoassay for the detection of angiotensin I in plasma using AlphaLISA acceptor beads technology," Anal. Biochem. **388**(1), 134–139 (2009).
22. J. Brown, L. Theis, L. Kerr, N. Zakhidova, K. O'Connor, M. Uthman, Z. M. Oden, and R. Richards-Kortum, "A hand-powered, portable, low-cost centrifuge for diagnosing anemia in low-resource settings," Am. J. Trop. Med. Hyg. **85**(2), 327–332 (2011).
23. A. P. Wong, M. Gupta, S. S. Shevkoplyas, and G. M. Whitesides, "Egg beater as centrifuge: isolating human blood plasma from whole blood in resource-poor settings," Lab Chip **8**(12), 2032–2037 (2008).
24. A. J. Mach, J. H. Kim, A. Arshi, S. C. Hur, and D. Di Carlo, "Automated cellular sample preparation using a Centrifuge-on-a-Chip," Lab Chip **11**(17), 2827–2834 (2011).
25. N. M. Pham, "Blood filtration for multiplexed point-of-care diagnostic devices," (University of Toronto, 2012).
26. C. Galli, "Modeling systematic errors: polychromatic sources of Beer-Lambert deviations in HPLC/UV and nonchromatographic spectrophotometric assays," J. Pharm. Biomed. Anal. **25**(5-6), 803–809 (2001).
27. O. P. Kristiansen and T. Mandrup-Poulsen, "Interleukin-6 and diabetes: the good, the bad, or the indifferent?" Diabetes **54**(Suppl 2), S114–S124 (2005).
28. H. Kugisaki, M. Sonohata, M. Komine, K. Tsunoda, S. Someya, H. Honke, M. Mawatari, and T. Hotokebuchi, "Serum concentrations of interleukin-6 in patients following unilateral versus bilateral total knee arthroplasty," J. Orthop. Sci. **14**(4), 437–442 (2009).
29. D. Mokart, M. Merlin, A. Sannini, J. P. Brun, J. R. Delpero, G. Houvenaeghel, V. Moutardier, and J. L. Blache, "Procalcitonin, interleukin 6 and systemic inflammatory response syndrome (SIRS): early markers of postoperative sepsis after major surgery," Br. J. Anaesth. **94**(6), 767–773 (2005).
30. H. Knüpfer and R. Preiss, "Significance of interleukin-6 (IL-6) in breast cancer (review)," Breast Cancer Res. Treat. **102**(2), 129–135 (2007).
31. V. W.-S. Wong, J. Yu, A. S.-L. Cheng, G. L.-H. Wong, H.-Y. Chan, E. S.-H. Chu, E. K.-O. Ng, F. K.-L. Chan, J. J.-Y. Sung, and H. L.-Y. Chan, "High serum interleukin-6 level predicts future hepatocellular carcinoma development in patients with chronic hepatitis B," Int. J. Cancer **124**(12), 2766–2770 (2009).
32. A. Hobisch, I. E. Eder, T. Putz, W. Horninger, G. Bartsch, H. Klocker, and Z. Culig, "Interleukin-6 regulates prostate-specific protein expression in prostate carcinoma cells by activation of the androgen receptor," Cancer Res. **58**(20), 4640–4645 (1998).
33. J. Y. Blay, S. Negrier, V. Combaret, S. Attali, E. Goillot, Y. Merrouche, A. Mercatello, A. Ravault, J. M. Tourani, and J. F. Moskovtchenko, "Serum level of interleukin 6 as a prognosis factor in metastatic renal cell carcinoma," Cancer Res. **52**(12), 3317–3322 (1992).
34. A. E. Flinterman, E. van Hoffen, C. F. den Hartog Jager, S. Koppelman, S. G. Pasmans, M. O. Hoekstra, C. A. Bruijnzeel-Koomen, A. C. Knulst, and E. F. Knol, "Children with peanut allergy recognize predominantly Ara h2 and Ara h6, which remains stable over time," Clin. Exp. Allergy **37**(8), 1221–1228 (2007).
35. S. H. Sicherer, A. Muñoz-Furlong, J. H. Godbold, and H. A. Sampson, "US prevalence of self-reported peanut, tree nut, and sesame allergy: 11-year follow-up," J. Allergy Clin. Immunol. **125**(6), 1322–1326 (2010).
36. A. M. Branum and S. Lukacs, *Food allergy among US children: trends in prevalence and hospitalizations* (US Department of Health and Human Services, Centers for Disease Control and Prevention, National Center for Health Statistics, 2008).
37. A. M. Szczepanik, L. Scislo, T. Scully, E. Walewska, M. Siedlar, P. Kolodziejczyk, M. Lenart, M. Rutkowska, A. Galas, A. Czupryna, and J. Kulig, "IL-6 serum levels predict postoperative morbidity in gastric cancer patients," Gastric Cancer **14**(3), 266–273 (2011).
38. S. L. Taylor, R. W. Crevel, D. Sheffield, J. Kabourek, and J. Baumert, "Threshold dose for peanut: risk characterization based upon published results from challenges of peanut-allergic individuals," Food Chem. Toxicol. **47**(6), 1198–1204 (2009).
39. A. Pomés, R. M. Helm, G. A. Bannon, A. W. Burks, A. Tsay, and M. D. Chapman, "Monitoring peanut allergen in food products by measuring Ara h 1," J. Allergy Clin. Immunol. **111**(3), 640–645 (2003).

#212166 - $15.00 USD Received 15 May 2014; revised 28 Aug 2014; accepted 29 Sep 2014; published 1 Oct 2014

40. S. L. Taylor, D. A. Moneret-Vautrin, R. W. Crevel, D. Sheffield, M. Morisset, P. Dumont, B. C. Remington, and J. L. Baumert, "Threshold dose for peanut: Risk characterization based upon diagnostic oral challenge of a series of 286 peanut-allergic individuals," Food Chem. Toxicol. **48**(3), 814–819 (2010).
41. A. E. Flinterman, S. G. Pasmans, M. O. Hoekstra, Y. Meijer, E. van Hoffen, E. F. Knol, S. L. Hefle, C. A. Bruijnzeel-Koomen, and A. C. Knulst, "Determination of no-observed-adverse-effect levels and eliciting doses in a representative group of peanut-sensitized children," J. Allergy Clin. Immunol. **117**(2), 448–454 (2006).
42. S. H. Sicherer and H. A. Sampson, "Peanut allergy: emerging concepts and approaches for an apparent epidemic," J. Allergy Clin. Immunol. **120**(3), 491–503 (2007).
43. M. Wensing, A. H. Penninks, S. L. Hefle, S. J. Koppelman, C. A. F. M. Bruijnzeel-Koomen, and A. C. Knulst, "The distribution of individual threshold doses eliciting allergic reactions in a population with peanut allergy," J. Allergy Clin. Immunol. **110**(6), 915–920 (2002).
44. G. A. Zurzolo, K. J. Allen, S. L. Taylor, W. G. Shreffler, J. L. Baumert, M. L. Tang, L. C. Gurrin, M. L. Mathai, J. A. Nordlee, A. Dunngalvin, and J. O. B. Hourihane, "Peanut Allergen Threshold Study (PATS): validation of eliciting doses using a novel single-dose challenge protocol," Allergy Asthma Clin. Immunol. **9**(1), 35 (2013).
45. J. M. Bland and D. G. Altman, "Statistical methods for assessing agreement between two methods of clinical measurement," Lancet **327**(8476), 307–310 (1986).
46. M. Enders, U. Bartelt, F. Knotek, K. Bunn, S. Strobel, K. Dietz, and G. Enders, "Performance of the Elecsys Rubella IgG assay in the diagnostic laboratory setting for assessment of immune status," Clin. Vaccine Immunol. **20**(3), 420–426 (2013).
47. N. Crofts, W. Maskill, and I. D. Gust, "Evaluation of enzyme-linked immunosorbent assays: a method of data analysis," J. Virol. Methods **22**(1), 51–59 (1988).
48. J. M. Bland and D. G. Altman, "Measuring agreement in method comparison studies," Stat. Methods Med. Res. **8**(2), 135–160 (1999).

1. Introduction

Medical diagnostics has grown into a burgeoning 48.5 billion dollar market with significant growth expected due to the implementation of the Affordable Care Act [1]. Combined with the anticipated shortage in clinical physicians [2], the importance of providing accessible point-of-care testing (POCT) technologies is rapidly increasing. Recent developments in POCT have been widely demonstrated across multiple clinical fields and in certain cases such as diabetes testing, have quickly moved into the realm of every-day life. POCT is expected to extend to important applications beyond human health diagnostics, including food safety, food processing quality control, water quality monitoring, animal diagnostics, and pathogen detection [3–6].

An important prerequisite for the widespread adoption of POCT is the availability of detection instruments that are inexpensive, portable, and able to share data wirelessly over the internet. Due to the rapid development of computational, communication, and sensing capabilities of smartphones since the introduction of the iPhone in 2007, these devices have become more like personal computers with integrated cameras, geolocation capabilities, and access to the internet. Since 2011, over 478 million smartphones are sold annually, with that number expected to double in the next 4 years [7], making them a nearly ubiquitous tool that can be adapted to performing POCT. Recent examples include attachments that enable smartphones to serve as stethoscopes [8], ultrasound probes [9], microscopes [10], fluorescent microscopes [11], and label-free biosensor detection instruments [12]. However, none of these techniques are able to address the need of liquid phase, spectrally-resolved absorption measurements required for many quantitative colorimetric tests, such as the Enzyme-Linked Immunosorbent Assay (ELISA).

Since its introduction 40 years ago, ELISA has become one of the most widely adaptable tools for biological assays, allowing for the rapid quantification of proteins and antibodies for diseases ranging from HIV to cancer, yielding over 40,000 new articles involving the technology annually [13].

An ELISA test is completed by immobilizing antibodies that possess an affinity for a specific biomolecule of interest onto a standard format 96-well microtiter plate and then passing over a series of liquids, exploiting the high specificity of the antibody-antigen interaction to yield a colorimetric change of the liquid sample based upon the cleavage of a chromogen moiety. After the optical absorptions of standards at known concentrations are used to obtain a calibration curve, the concentrations of an analyte within a test sample may be accurately determined via interpolation.

#212166 - $15.00 USD Received 15 May 2014; revised 28 Aug 2014; accepted 29 Sep 2014; published 1 Oct 2014

While colorimetric tests have been demonstrated utilizing various red-green-blue (RGB) color image weighting techniques to analyze biological molecules of interest by taking photographs of the sample [14–16], these mechanisms do not provide the spectrometric data required to perform an ELISA test. CMOS sensors, like those found in most smartphone devices, are wavelength-independent photon collectors that are converted into RGB pixels via physical filters. These filters are comprised of colored dyes that each have their own spectral response [17], and an additional infrared cutoff filter with a response that provides a sharp drop in transmittance that can vary even among batches of identical cameras by 10 nm [18]. In such a system, light intensity and color are intrinsically intertwined as they both rely on the number of photons captured by the RGB pixels compared to that of their adjacent neighbors. By dispersing the spectrum of absorbed light along one of the CMOS camera dimensions, we are able to determine the wavelength-specific absorbance of samples, enabling accurate analysis of ELISA tests.

Here, we demonstrate the use of a smartphone to perform the readout and quantification of any ELISA assay, and compare results with those obtained from a conventional laboratory-bench ELISA microplate reader for two unrelated biomarkers, representing both the universality of the device to work with different ELISA based biological assays and the immediate utility of the technology in both clinical and commercial settings. First, we demonstrate smartphone-based detection of a clinical biomarker in serum used for human disease diagnostics. Second, we demonstrate detection of a peanut allergen in the context of a food safety application. While these two tests cannot serve as a complete representation of the hundreds of existing ELISA kits that the technology can be integrated with, they are dissimilar enough to demonstrate the expected universality of a new measurement modality that provides comparable results with those of a conventional bench reader without modifying existing ELISA procedures. While there have been successful demonstrations of simplifying liquid handling steps [19–21] and both macro- and microfluidic sample collection techniques amenable to POCT [22–25], high quality spectroscopic instruments have yet to be developed for on-site analysis. By providing a spectroscopic reader for ELISA tests that is integrated with a mobile communication device, this technology can be used on the myriad of existing, well-studied ELISA procedures that have been well characterized for spectroscopic-based analysis. Combined with approaches for microfluidic-based automation of sample preparation procedures, the detection instrument approach presented in this work opens up the possibility of transferring ELISA-type tests to other fields requiring point of care analysis, such as quality control validation and agricultural monitoring. In this paper we will demonstrate the comparative robustness and sensitivity of a smartphone-based ELISA reader, and pose a method for further increased sensitivity via use of integrative spectral measurement.

2. Methods

2.1 Optical setup

The instrument is designed to interface with an iPhone 4 (800 MHz ARM Cortex A8, Omnivison OV5653 5MP BSI CMOS sensor with f/2.4, 5 element lens; Apple Inc.) by using the onboard, rear-facing camera as a digital light detector. A custom cradle fabricated from anodized aluminum was designed to align the necessary optics with the phone camera as described previously [12], enabling the camera to function as a spectrometer. A schematic diagram of the smartphone detection system is shown in Fig. 1.

#212166 - $15.00 USD Received 15 May 2014; revised 28 Aug 2014; accepted 29 Sep 2014; published 1 Oct 2014

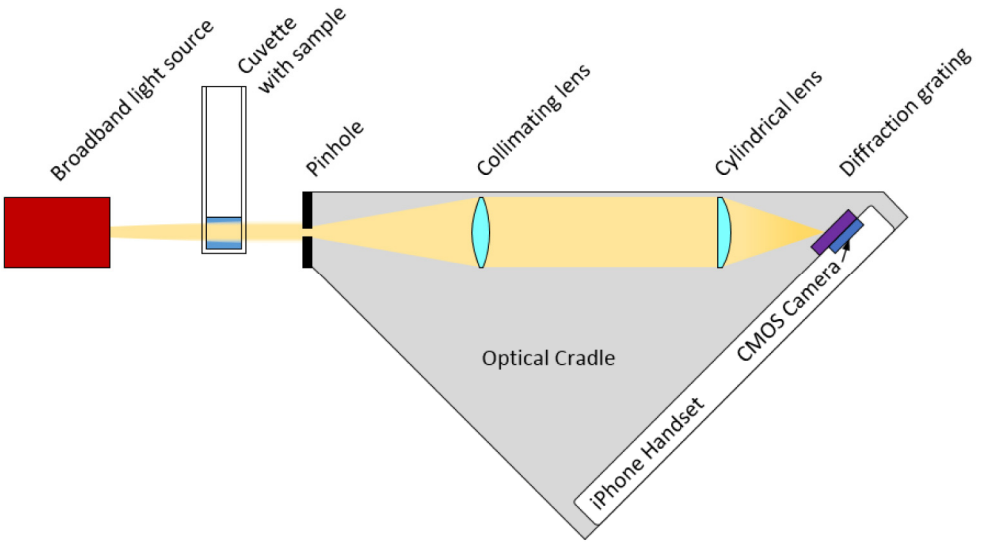

Fig. 1. Schematic of the smartphone-based absorption detection system. A broadband light source illuminates a cuvette containing a sample solution (food coloring dye, biological molecule). The solution absorbs specific wavelengths in the visible range. The transmitted light emerges from the cuvette passes through a 0.1 mm diameter pinhole and enters the isolated optical cradle. The light is then collimated, focused into a line, and passed through a diffraction grating before being collected by the on-board CMOS sensor of the smartphone.

A broadband light source (150 W halogen fiber optic high intensity illuminator; Cole Parmer) is used to illuminate the sample cuvette. Light that is not absorbed by the sample is collected by a 1 mm diameter optical fiber and relayed to a 0.1 mm diameter pinhole. Light that enters the optical chamber is collimated and focused to a line by a cylindrical lens (focal length = 50 mm), and passed through a diffraction grating (1200 grooves/mm; Edmund Optics) at an angle of ~47 degrees to direct the first-order diffracted light onto the CMOS sensor of the smartphone. The wavelength components of the light are separated by the diffraction grating, which disperses the light onto the pixels of the camera. Illumination from the lamp is observed in the resulting camera image as a bright, rainbow band appearing near the center of the screen on the smartphone. The camera resolution (2592 × 1936 pixels) and the dispersion of the diffraction grating combine to provide a spectral resolution of 0.334 nm/pixel along the spectral axis of the resulting image.[2] The width of the band along the direction orthogonal to the dispersion in image is determined by the diameter of the pinhole, and is approximately 100 pixels across. Due to the spectral responsivity of the Si-based sensor and internal infrared cutoff filters within the camera optics, the range of wavelengths which may be observed by the system extends from approximately 400 to 700 nm.

2.2 Use of the smartphone instrument

Before introduction to the smartphone instrument, the iPhone was prepared by first locking the focus and exposure of the native camera application by focusing on a point sufficiently far away in a dark room/hallway to focus the camera at an infinite distance. The phone was then placed in the cradle, and a broadband illumination source was turned on at the end of the optical path. The phone was aligned using adjustment knobs to achieve an x-y positioning providing a centered image of a broadband spectrum on the smartphone display. For every measurement step, five consecutive images were captured using the native iPhone camera application, and averaged to account for variations arising from the camera hardware. Red and green laser pointers (λ = 656.26 nm and λ = 532.10 nm, respectively) measured with a spectrometer (USB2000 + ; Ocean Optics) were imaged using the smartphone system, and

#212166 - $15.00 USD Received 15 May 2014; revised 28 Aug 2014; accepted 29 Sep 2014; published 1 Oct 2014

their emission profiles were fit with a 4th order polynomial curve to determine the pixel-to-wavelength conversion, found to be 0.334 nm/pixel (Fig. 2).

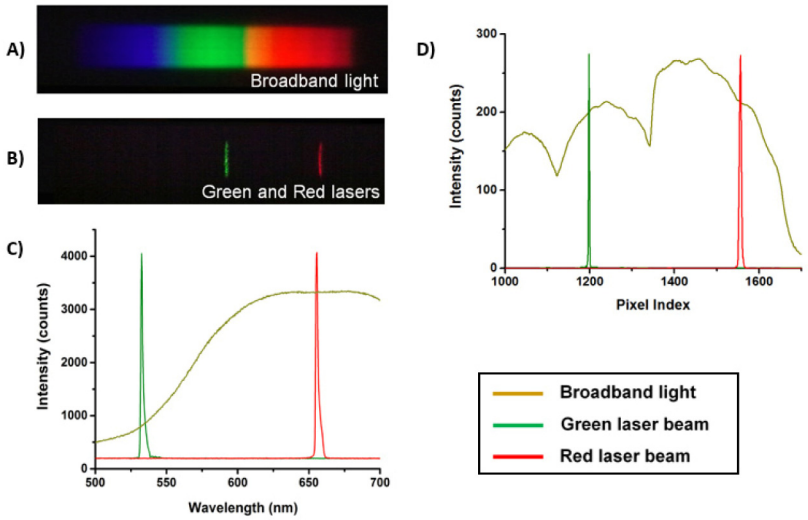

Fig. 2. Raw images of broadband (**A**), and laser illumination (**B**) collected on the smartphone system. **C.** Spectra from the two lasers and a broadband light source measured by a spectrometer **D.** The processed spectra of the lasers and broadband spectrum from the smartphone used for pixel-wavelength calibration.

2.3 Digital image analysis

Post-processing scripts were written in Matlab to convert raw images into absorption spectra. First, auto-thresholding is performed to crop non-data pixels from analysis by removing pixels with zero intensity, which yields a reduction of the image to a ~1100 x 100 block of pixels. The intensity of pixels in the non-spectral direction are averaged to yield a one-dimensional vector representation of the spectra. Pixel values are converted to wavelength values using a linear approximation via known pixel indices calculated by illuminating the pinhole with red and green laser pointers, as described previously [12]. As the entirety of chromogenic spectral data for *3,3′,5,5′* trimethylbenzidine (TMB) tests is captured solely in the blue channel of the RGB data, red and green channels are omitted from further calculation for ELISA-based measurements. To generate absorption spectra, converted vector forms of the data were subtracted from those of a blank comprised of deionized (DI) water, and normalized to the RGB response of the sensor when illuminated without sample or cuvette present in the optical path.

To best compare the smartphone measurement sensitivity to that of a commercially available microplate reader, absorption values at $\lambda = 450$ nm are interpolated from calibrated spectra. In addition, recognizing the potential value of the full spectral data for each sample, we calculate the integrative absorption from $410 < \lambda < 500$ nm (Fig. 3). Finally, the ELISA microplate reader data is imported directly from the output data files, appropriately normalized to the blank, and averaged across.

#212166 - $15.00 USD Received 15 May 2014; revised 28 Aug 2014; accepted 29 Sep 2014; published 1 Oct 2014

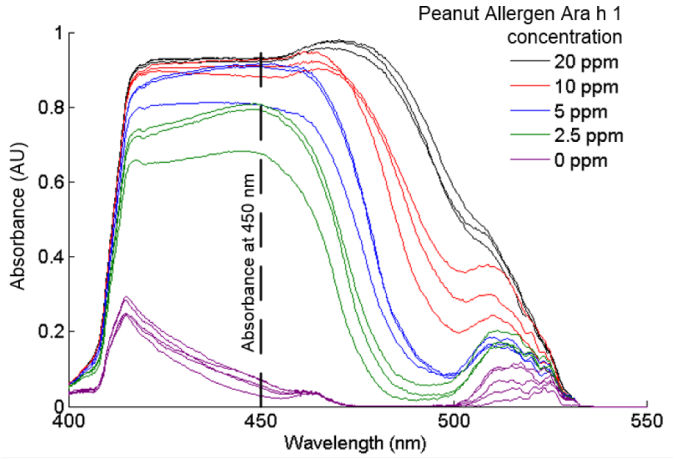

Fig. 3. Example of Wavelength-Normalized Spectra Generated from Camera Images with Peanut Allergen Ara h 1. Five independent smartphone images were averaged, then normalized to a blank. Using lasers of known wavelength, images were converted to wavelength-dependent spectral absorbances. Five concentrations of peanut allergen Ara h 1 are present to illustrate the difference in absorption characteristics. The dashed line at $\lambda = 450$ nm represents the single wavelength at which conventional ELISA measurements are taken using a microplate reader.

For each measurement method, the absorption as a function of concentration for the calibration standards is fit to a four parameter logistic regression model based upon an expected sigmoidal response curve governed by Eq. (1):

$$F(x) = D + \frac{A - D}{1 + \left(\frac{x}{C}\right)^{B}} \qquad \text{Eq. (1)}$$

where A is the minimum asymptote, B is the Hill's slope, C is the inflection point, and D is the maximum asymptote. While Beer-Lambert relations are often used to characterize absorption-based measurements this logistic model was selected both on the recommendations of the assay protocols and to account for sensor saturation effects and polychromaticity for integrative absorption measurements [26]. Limits of detection are calculated as three standard deviations above the average zero-concentration value for each measurement method.

3. Results

3.1 Preliminary colorimetric dye measurements

By providing full visible spectral measurements, the smartphone instrument can analyze a wide range of colorimetric moieties including fluorescent chemical compounds, conventional dyes, and complex biological fluids that absorb or emit light preferentially at various wavelengths. To demonstrate proof-of-concept for our smartphone based absorption measurement system, the spectral profiles and concentration dependencies of commercial food coloring dyes were measured (McCormick Inc.). Light transmitted through the solution provided unique absorption profiles resulting from the dyes.

#212166 - $15.00 USD Received 15 May 2014; revised 28 Aug 2014; accepted 29 Sep 2014; published 1 Oct 2014

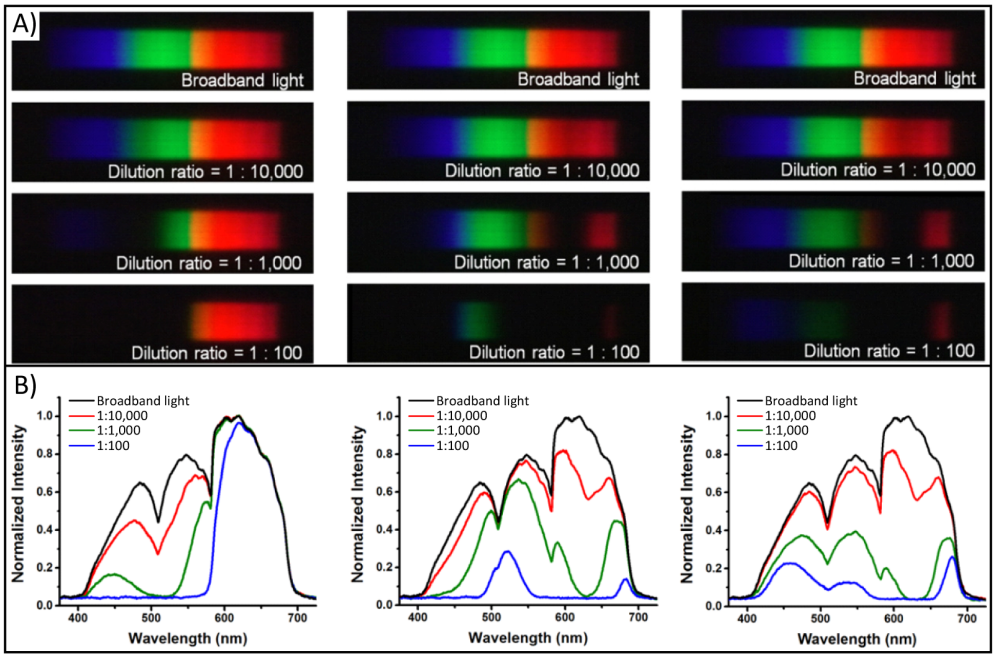

Fig. 4. Spectral analysis of food coloring dyes. A). Red, green, and blue food coloring dyes were diluted 100 x-10,000 x and measured using the smartphone instrument. Dark bands in the characteristic 'rainbow' band correspond to wavelengths of light absorbed by the dyes, and B) are easily identifiable once converted to one-dimensional vectors of spectral intensity (bottom).

Experimentally obtained spectral profiles of three different dyes (red, green, blue) are presented in Fig. 4. Dyes were diluted 1:100, 1:1,000, and 1:10,000 in DI water to characterize the concentration-dependence of the absorption spectra. A standard polystyrene cuvette (10 mm optical path; Globe Scientific) filled with DI water was used to normalize the RGB intensity values during image post-processing. For each food coloring dye measurement, the cuvette was filled with 1 ml of solution and placed into a holder. When broadband light passes through the food coloring solution, specific wavelengths are absorbed by the dye as shown by dark bands in the spectra in Fig. 4(A). From these images, one-dimensional spectral intensity profiles were generated and then normalized to the maximum intensity value. The smartphone detection system successfully measured differences in absorption even between samples that are indistinguishable by visual inspection. As expected, a concentration-dependence was observed with each dye absorbing maximally in the region of the spectrum near the color of its visual appearance.

3.2 IL-6 assay

Human Interleukin-6 (IL-6) is an important cytokine involved in the signaling cascade for the pro-inflammatory activation of B-cells following T-cell activation from an antigen-mediated immune response. Elevated expression of IL-6 in serum samples has been demonstrated as an important indicator in conditions ranging from diabetes to postoperative surgical stress [27–29]. Additionally, IL-6 has been shown to be a relevant cancer biomarker important for the tracking, classification, and prognosis of various cancers including breast, hepatic, prostate, and renal varieties [30–33].

A commercially available ELISA kit was purchased (Invitrogen) for the quantification of human IL-6. Lyophilized IL-6 was reconstituted in standard diluent buffer, and serially diluted to concentrations of 128, 64, 32, 16, 8, 4 and 2 pg/mL. Standards were added to pre-prepared wells with immobilized anti-IL-6 antibodies in duplicate (n = 2). Reconstituted IL-6 was then serially diluted in fetal bovine serum (FBS, Sigma) to demonstrate the specificity of

#212166 - $15.00 USD Received 15 May 2014; revised 28 Aug 2014; accepted 29 Sep 2014; published 1 Oct 2014

the ELISA test in the presence of interfering species. A blank well was incubated with only diluent buffer. Biotinylated anti-IL-6 antibody was added to each well, and the solutions were allowed to incubate, covered, for 2 hours at room temperature on an orbital shaker (100 rpm). Solutions were removed, and the wells were rinsed (4x) with the provided wash solution, per assay instructions. Streptavidin-HRP solution was added to each well, and the plate was returned to the shaker for another 30 minutes. Another wash step was completed as before, and 100 μL chromogen solution (TMB) was added to each well. The plate was then incubated for 10 minutes in the dark, before applying an equal amount of provided stop solution.

Using a commercially available ELISA microplate reader (BioTek Synergy HT), the completed assay was measured for absorbance at 450 nm, and blanked against a control well. Afterward, samples were individually transferred to polystyrene cuvettes that were placed in a cuvette holder fixed permanently in the optical path to minimize variation due to geometric inconsistencies. A cuvette filled with 200 μL deionized water was used to normalize the RGB intensity values during image post-processing.

After data processing, the captured images were converted to absorption spectra that show clear concentration dependence across a range of wavelengths from 400 to 550 nm. From these spectra, either single wavelength measurements, akin to a microplate reader, or integrative absorption measurements can be calculated. After digital data analysis, both standard and spiked IL-6 concentrations were observed to follow a sigmoidal dose-response curve, as expected (Fig. 5). From the data collected, it can be observed that the smartphone-based absorption at 450 nm as well as the integrative absorption replicate the microplate reader measurements throughout the entire range of standard concentrations, validating our instrument as a portable, low-cost alternative to traditional benchtop apparatus. The limits of detection observed were in line with the manufacturer's specified limit for the assay of 2 pg/mL. Spiked bovine serum samples were analyzed with both the commercially available benchtop microplate reader and the smartphone system, and strong agreement was observed for both techniques, as demonstrated via Bland-Altman analysis (Appendix).

#212166 - $15.00 USD Received 15 May 2014; revised 28 Aug 2014; accepted 29 Sep 2014; published 1 Oct 2014

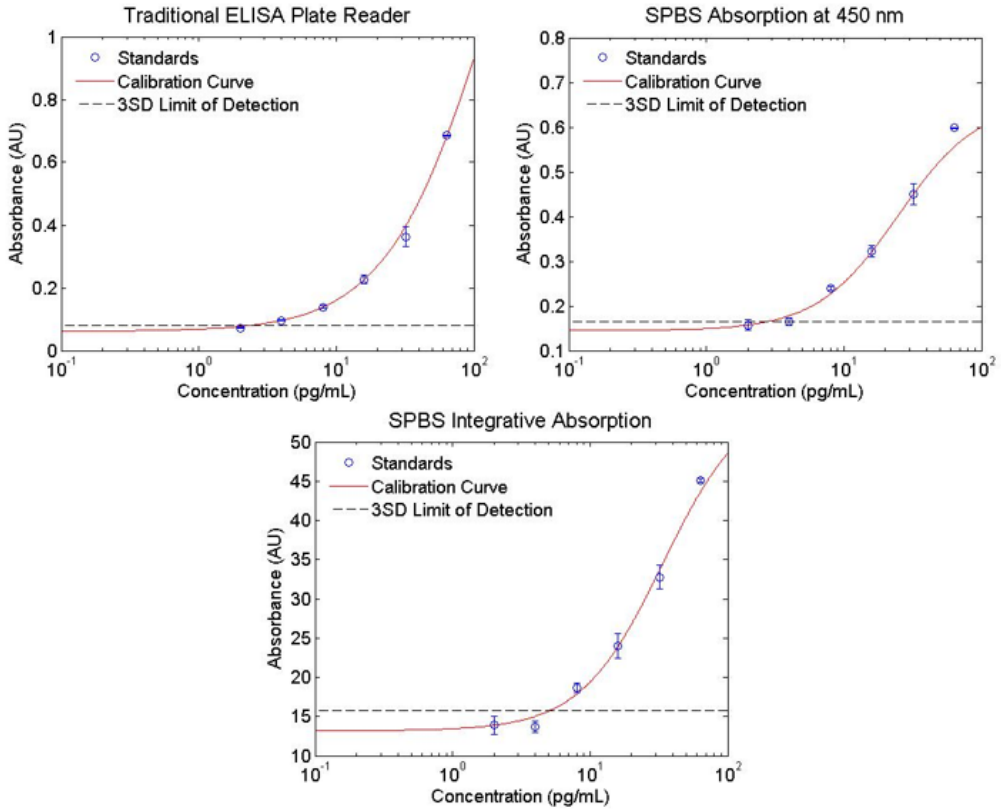

Fig. 5. Concentration Dependence of Human IL-6. Samples were measured by an ELISA microplate reader, and then transferred to cuvettes to be measured by the smartphone instrument. Concentrations ranging from 2.0 pg/mL to 125 pg/mL were measured (n = 2) along with a 0 pg/mL control (n = 3). Calculations of the data collected by the smartphone were completed both at 450 nm, so as to be directly comparable to conventional ELISA data, and as the integrative absorption from 410 <λ< 500 nm. Limits of detection were calculated as three standard deviations above the 0 concentration measurement average.

3.3 Peanut allergen detection

The Ara group of peanut proteins consist of those that elicit allergic responses. While the specific proteins that an individual might be allergic to might vary, between 70% and 90% of individuals allergic to peanut products produce an immune response to the proteins Ara h 1, Ara h 2, and Ara h 6, a homolog for Ara h 2 [34]. In the US, over 1% of individuals have a self-reported peanut allergy, and this rate seems to be increasing in children [35]. While many precautions exist to assist those with severe allergies to avoid peanut-based products, there is an increasing trend in the number of peanut allergy-related hospitalizations each year [36]. There is a high potential value in a portable smartphone-based test for peanut allergens present in food, but careful quantification is absolutely essential. To our knowledge, this work presents the first proof-of-concept of a portable peanut assay that is capable of measuring peanut at concentrations less than the smallest measured No Observed Adverse Effect Levels (NOAELs).

A commercially available ELISA kit was purchased (R-Biopharm) for the quantification of peanut allergens Ara h1 and Ara h2. Samples were taken from cookies purchased from two local bakeries, Insomnia Cookies, and Schnuck's Grocer, as well as from pre-packaged vanilla Oreo® cookies. Samples were extracted per kit instructions: 1 gram of each cookie sample was ground and placed in a solution of extraction buffer diluted from the provided 10x concentrate. Extraction was completed at 60°C for 10 minutes, followed by a 10 minute

#212166 - $15.00 USD Received 15 May 2014; revised 28 Aug 2014; accepted 29 Sep 2014; published 1 Oct 2014

centrifugation at 2,500 g. The supernatant was then incubated, along with calibrated concentrations of peanut solution, in 400 μL wells with immobilized anti-Ara h 1 antibodies in triplicate. Enzyme conjugate, chromogen, and stop solutions are then added for 10 minutes each, with a 3x wash step in between. The entire process can be completed in under an hour.

The same preparation protocol developed for the IL-6 assay was again used for the Ara h 1/2 assay. The spectra were normalized to a water-filled cuvette during post-processing, and positioning was repeated. Lasers were used to recalibrate, and samples were measured in a similar fashion. After digital data analysis, standard Ara h 1/2 concentrations were also observed to follow a sigmoidal dose-response curve (Fig. 6). The limits of detection for the reported peanut assays were between 0.09 and 0.56 ppm. Once again, comparative validation was completed with a microplate reader (Appendix). Samples from peanut-containing cookies were found to have absorbances over that of the maximally assayed standard concentration (20 ppm), and so could not be quantitatively measured without further dilution. While neither Insomnia nor Schnuck's claimed that their sugar cookies were safe for consumption by people with peanut allergies, the sugar cookie from Schnuck's did, in fact, have an absorbance less than the assayed limit of detection (Fig. 7). As expected, prepackaged sandwich crackers without a label indicating a risk of nut contamination tested below the LOD.

3.4 Comparison of smartphone sensitivity and ELISA microplate reader

For each sample measured in the conventional microplate reader, a spectrum was generated from a series of 5 collected images. Both the absorption at $\lambda = 450$ nm and the integrative absorption from $\lambda = 410$ to 500 nm were calculated. All data points were fit with the same four-parameter logistic model described above. From the data collected, the absorptive LOD from either sensing modality appear to be in rough concordance, whereas the LOD obtained using the integrative absorption method is consistently 2-3x lower (Table 1) than that obtained by considering the absorption of only a single wavelength. This suggests that by taking advantage of the full spectral profile of the absorption from the chromogen, it is possible to achieve a higher sensitivity than that obtained by observing a single wavelength. The availability of the full spectral absorption information also enables the system to easily function with a broad range of chromogens that generate different colored solutions.

#212166 - $15.00 USD Received 15 May 2014; revised 28 Aug 2014; accepted 29 Sep 2014; published 1 Oct 2014

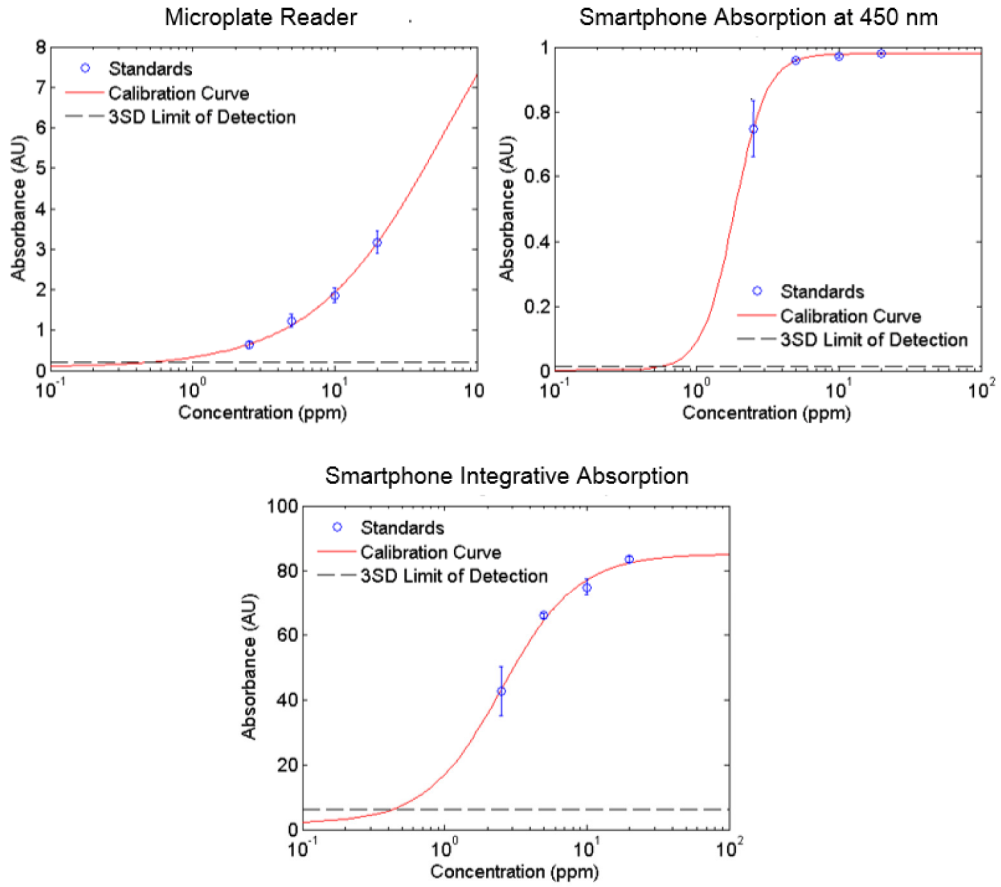

Fig. 6. Concentration Dependence of Ara h 1. Samples were measured by an ELISA microplate reader, and then transferred to cuvettes to be measured by the smartphone instrument. Concentrations ranging from 2.5 ppm to 20 ppm were measured along with a 0 ppm control (n = 3). Calculations of the data collected by the smartphone were completed both at 450 nm, so as to be directly comparable to the output of the ELISA microplate reader data, and as the integrative absorption from 410 to 500 nm. Limits of detection were calculated as three standard deviations above the 0 concentration measurement average.

4. Discussion

The diagnostic potential for biomarkers such as IL-6 is significant. Tracking the post-operative serum levels of biomolecules to assess the chances of post-operative complications could potentially increase positive outcomes for those patients via early-detection [29], and decrease required post-operative in-hospital recovery time. While long-term monitoring of biomarkers could likely provide valuable prognostic information, the associated load on hospitals and diagnostic laboratory facilities make any such testing at best expensive, and at worst, unrealistic. Similarly, the measurement of cancer-related biomarkers might prove a useful tracking mechanism for potential relapse or metastatic risk [37]. The development of a cheap yet reliable ELISA reader could facilitate the development of a broadly available test in clinic-type environments.

#212166 - $15.00 USD Received 15 May 2014; revised 28 Aug 2014; accepted 29 Sep 2014; published 1 Oct 2014

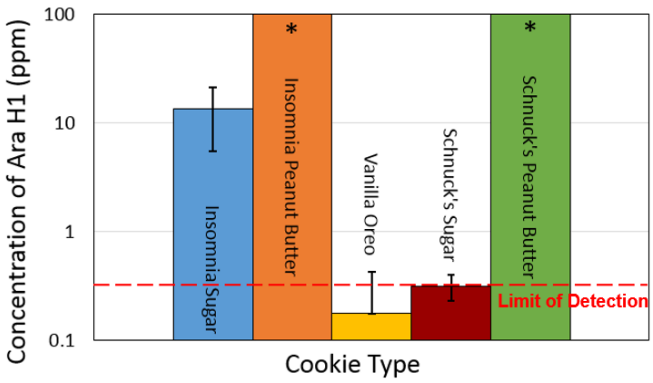

Fig. 7. Quantification of Ara h 1 in Cookie Samples from Two Local Bakeries. Sample cookies were collected and contained separately in plastic to avoid cross-contamination. Samples were measured, ground, and proteins were extracted following manufacturer protocol. Vanilla Oreo® samples (n = 3) and Schnuck's cookie samples (n = 2) were assayed with data in Fig. 6, and Insomnia cookies were assayed with data from a similar experiment (data not shown). As the cookies were run on two different assays, only the higher LOD is shown. * Peanut Butter cookies had concentrations of Ara h 1 higher than the maximum assayed standard concentration, so significant dilution would be required for accurate quantification.

Table 1. Comparison of detection limits of the Ara h 1 ELISA microplate reader, smartphone absorption at λ = 450nm, and smartphone integrative absorption.

	ELISA Microplate reader	Smartphone Absorption at 450 nm	Smartphone Integrative Absorption
Experiment 1	**0.314 ppm**	**0.268 ppm**	**0.107 ppm**
Experiment 2	**0.529 ppm**	**0.560 ppm**	**0.269 ppm**

At the other end of the spectrum from laboratory-based medical diagnostics, allergen detection provides a consumer-based testing opportunity, just one of many examples of the broad applicability of a smartphone-based instrument capable of reading any type of ELISA test. While existing microplate readers are prohibitively expensive for individuals and designed specifically for laboratory settings, a handheld smartphone attachment is naturally amenable to an in-home testing environment. While reagent costs are non-trivial (the kit used in this work had a per-sample cost of $10), as consumer-targeted kits, there is significant potential for material cost reduction via both the future miniaturization of the liquid handling system and partnership with an existing biologics manufacturer. By decreasing the cost of the detection instrument, and broadening the situations in which it might be used, the developed smartphone-based biosensor addresses one of the principle costs of performing laboratory-based ELISA tests. Though ELISA assays require multiple liquid-handling steps, there have already been several successful demonstrations of ELISA performed as a lab-on-a-chip technique that could be integrated into a low cost, disposable cartridge, readily read by an instrument such as the one described here. While significant work has gone into simplifying both the sample collection process and the liquid handling steps used in a traditional ELISA test, there is a significant, unmet need for an instrument that can replicate the accuracy and repeatability of a microplate reader in a point-of-care system that can complement these advances.

Current alternatives for assay readout are based on either visual inspection or non-spectral image analysis, neither of which provide the spectral resolution of traditional microplate readers. ELISA testing is dependent on this spectral resolution, as the chromogens that are being measured are characterized by non-uniform absorption spectra in the visible range. Non-spectral methods of color analysis are subject to the variations in intensity present across various wavelengths, usually binned into three RGB channels via a Bayer filter. While it is possible to account for wavelength-dependent absorption via normalization with two- or

#212166 - $15.00 USD Received 15 May 2014; revised 28 Aug 2014; accepted 29 Sep 2014; published 1 Oct 2014

three- band illumination, it requires hardware-based filtering, which would need to be changed out for each chromogen being measured. By diffracting the wavelength of transmitted light along one of the physical dimensions of the CMOS sensor, we are able to separate the intensity information of the absorbed light from its wavelength, thereby allowing for the wavelength-specific quantification of chromogenic absorption. While filter-based multi-band illumination may be cheaper for individual applications, our spectrometric reader is capable of providing universal flexibility to read chromogens across all visible wavelengths of the spectrum, even in regions where RGB channels overlap, including both 450 and 492 nm, wavelengths where the important ELISA chromogens TMB and OPD maximally absorb, and where RGB analysis cannot suffice without switching out chromogen-specific filters.

While there is general consensus on the importance of minimizing peanut material in non-peanut-containing foods, surprisingly little work has been done to quantify the amount of peanut protein required to produce an allergic reaction in affected individuals. Literature review-based statistical modeling has produced a starting point for such efforts, but variations in testing modalities as well as an abundance of situations where NOAELs could not be determined due to observed allergic responses at the lowest assayed dosage have resulted in a large number of patient results being excluded [38, 39]. One of the most promising studies of existing data was collected from clinical records of patients being tested, rather than from specific patient-recruited studies, which yielded an eliciting dose in 5% of the population (ED_5) of 4.2 mg peanut protein [40]. While there is uncertainty in some of the numbers prevalent in the literature, the overall range of subjective NOAELs reported (or estimated) is typically between 0.4 and 10 mg protein [40–43], with objective ED_5 have been estimated as low as 1.5 mg [44]. For a reasonable maximal daily intake of 500g of food based upon a 2000-3000 calorie diet, this would translate to 0.8 and 3 ppm peanut protein for minimum reported NOAEL and ED_5, respectively, which are higher than the LOD for each of the testing methodologies used. Thus we have successfully demonstrated a point-of-use testing modality that can plausibly be used to measure clinically relevant amounts of peanut.

While this work has focused upon the demonstration of a liquid-based color absorption assay in the context of an ELISA, the approach demonstrated here may be applied to any assay that results in the color change of a liquid. Colorimetric tests are relatively common due to their ability to be qualitatively measured via visual inspection. Such tests are commonly used in testing liquids for pH, chlorination, and contaminants ranging from metals to organics. While qualitative information is useful, spectroscopic analysis is able to provide quantitative information that is consistent across phone manufacturers and independent of operator or hardware-based differences, a significant improvement over both visually comparative methods and non-spectrally resolved imaging methods. Broadly, this instrument can perform any such test, assuming the absorption spectra exists within the visible range of wavelengths.

5. Conclusion

We have demonstrated a smartphone-based spectroscopic ELISA detector that is capable of performing valuable clinical assays in a portable system. Using two commercially available ELISA reagents for detection of a disease biomarker and a food allergen, we demonstrated limits of detection that are identical to or better than those obtained with a conventional ELISA microplate reader. Furthermore, we demonstrated that the spectral information available by measuring the entire absorption spectra of the assay liquid can be used to achieve 2-3x lower limits of detection, compared to measuring the absorption at only a single wavelength. In addition to the benefits of portability and decreased cost, a smartphone ELISA platform also can make use of other smartphone capabilities, including immediate connectivity to the internet, geolocation, and has the potential for such results to be transmitted with medical records databases or even remotely located clinicians. Likely these capabilities can be further refined, and even translated to other spectroscopic assay modalities.

#212166 - $15.00 USD Received 15 May 2014; revised 28 Aug 2014; accepted 29 Sep 2014; published 1 Oct 2014

Appendix: validation of smartphone measurement technique vs. microplate reader

Bland-Altman plots for the IL-6 spiked FBS samples and Ara h 1 experiments are shown in Fig. 8. As ELISA absorbance measurements often have a lognormal distribution, a variation on the standard method using the geometric mean and log difference was applied to all non-zero values for each assay [45–47]. The log differences showed a dependence on the magnitude of the measurement, so a regressive approach was used to model the relation, as described by Bland and Altman (mean of regression shown with dashed line) [48]. As the relationship between the residuals and magnitude of the measurement was found to be significant, these values were also regressed against the magnitude of the measurement and combined with the first model to provide the 95% limits of agreement [48]. No points were found to be outside the ±1.96 S. D. limits of agreement (solid lines). These data demonstrate a high level of consistency between the conventional ELISA microplate reader and the smartphone-based spectroscopic absorbance measurements.

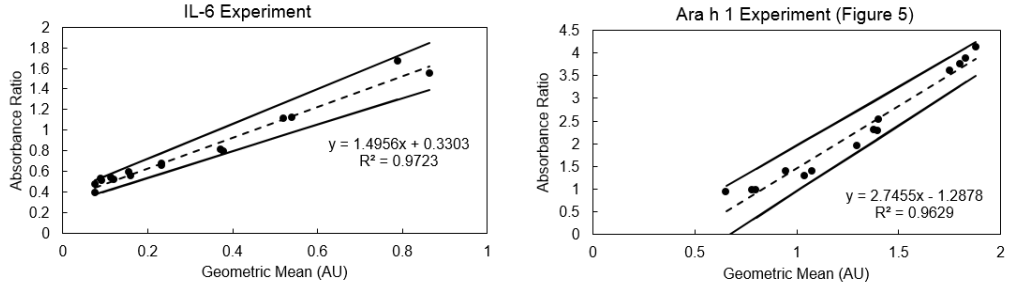

Fig. 8. Bland-Altman Analysis of smartphone instrument with traditional microplate reader.

Acknowledgments

We would like to acknowledge the National Science Foundation for their support of this work via Grant no. CBET 12-64377. Additionally, we would like to express our gratitude for the assistance of P.T. Clark for his assistance with the optical design calculations.